

LIMNOLOGY and OCEANOGRAPHY



Limnol. Oceanogr. 67, 2022, 1429–1442
© 2022 Association for the Sciences of Limnology and Oceanography.
doi: 10.1002/lno.12080

High-frequency pH time series reveals pronounced seasonality in Arctic coastal waters

Arley F. Muth ¹, ^{1*} Amanda L. Kelley ¹, ² Kenneth H. Dunton ¹

¹University of Texas Marine Science Institute, Port Aransas, Texas

Abstract

The accelerated rate of climate change in the Arctic Ocean occurs in conjunction with a system known for its extreme seasonal variability. Here, we present 2 years of continuous pH, salinity, and temperature data from the north Arctic coast of Alaska from instruments deployed in a kelp bed at 4.5–6 m depths in Stefansson Sound. At the innermost site, which receives freshwater runoff from the nearby Sagavanirktok River, short-term pH variability in late spring and summer produced pH values up to 8.67. The pH values of the deeper offshore site were less affected by freshwater input, although biological (heterotrophy) and physiochemical (ice formation) processes dominated during the winter months, driving pH down to 7.47 during the 8-month period of ice cover. These long-term physicochemical measurements reveal the natural but critical influence of changing river inputs on the pH of Arctic nearshore waters which support highly productive communities and subsistence fisheries.

High-latitude systems are most impacted by climate change as reflected by elevated sea surface temperature, increases in freshwater input, a 30% decrease in summer ice extent, and higher susceptibility to ocean acidification (Zhang 2005; Fabry et al. 2009; Morison et al. 2012; Meier et al. 2014). Ocean acidification, a process caused by an increase in atmospheric $\rm CO_2$ that is subsequently absorbed by the world's oceans, has decreased ocean pH values below pre-industrial levels (0.1 units; Wickett and Caldiera. 2003; Raven et al. 2005). As $\rm CO_2$ dissolves into seawater, carbonic acid forms, releasing hydrogen ions into the ocean and decreasing pH.

Ocean acidification has been shown to have complex, nonlinear impacts on marine organisms across taxa (Kroeker et al. 2010), with polar organisms particularly sensitive to low pH conditions (Kelley and Lunden 2017). Acidification rates are governed by physicochemical processes that vary widely from region to region (Bates et al. 2014), making it difficult to predict future changes in areas that are data-limited, especially in polar regions. CO₂ is more soluble in high-latitude, colder oceans, and prolonged periods of time dominated by heterotrophy (respiration) further increase CO₂ partial pressure

Additional Supporting Information may be found in the online version of this article.

Author Contribution Statement: A.F.M. contributed to the design, acquisition, analysis, interpretation of the data and writing. A.L.K. contributed to the analysis, interpretation of the data and writing. K.H.D. contributed to the design, acquisition, interpretation of the data and writing.

 (pCO_2) within the water column that decreases ocean pH (Fabry et al. 2009). In the Arctic, this process is exacerbated by large amounts of freshwater input, decreasing nearshore salinities and total alkalinity (Mathis et al. 2015).

To date, most pH and carbonate chemistry data reported from the Arctic Ocean are low-resolution and consist primarily of discrete ship-based bottle sampling efforts that are concentrated during periods of lower ice cover from late spring to autumn (Bates et al. 2009; Mathis et al. 2011, 2015). Freshwater input from ice melt and river runoff (Chierici and Fransson 2009; Yamamoto-Kawai et al. 2009), localized upwelling (Mathis et al. 2011), and anthropogenic CO_2 uptake (Bates et al. 2009) contribute to regional and temporal instances where waters are undersaturated with respect to aragonite. Low saturation levels of aragonite (Ω_{arag}), the most commonly reported calcium carbonate mineral, have direct repercussions on the ability of marine calcifying organisms to survive past their larval stages (Gangstø et al. 2008; Büdenbender et al. 2011; Diaz-Pulido et al. 2012).

At the land-sea interface, carbonate chemistry is highly dynamic, mainly driven by biophysical forcing that is absent in the open ocean (Carstensen and Duarte 2019). Drivers of pH variability in marginal seas are a result of seasonal freshwater input and photosynthesis and respiration, which can act on multiple time scales (hourly, daily and seasonal; Miller et al. 2018). Many nearshore marine environments are directly influenced by riverine waters which in turn affect saturation levels of aragonite as these waters have higher total alkalinity values than ice melt (Schneider et al. 2007; Cooper et al. 2008), which can have low total alkalinity, particularly fjord-sourced freshwater (Evans et al. 2014).

²University of Alaska Fairbanks, Fairbanks, Alaska

^{*}Correspondence: arley.muth@uteaxs.edu

Although the Arctic Ocean receives 11% of the world's freshwater run-off, it only contains ~ 1% of the world's ocean volume (McClelland et al. 2012), underscoring the impact that freshwater flux can have in the Arctic nearshore. Furthermore, most of this freshwater is released during a brief period each spring during the spring freshet, causing drastic changes to nearshore water stratification, composition, and chemistry. The Sagavanirktok (Sag) River, which is the second largest river draining the North Slope of Alaska (1.6 km³ annual discharge; McClelland et al. 2014), transects the Brooks Range and empties into Stefansson Sound. This intense, seasonal burst of freshwater to the nearshore marine ecosystem likely plays an important role in structuring biological communities via its direct impact on seawater physicochemical processes.

High-frequency pH data are important for understanding the severity and magnitude of future impacts of ocean acidification on the carbonate dynamics of nearshore environments. In addition, manipulative ocean acidification experiments can include present-day pH variability as a means to adequately frame organismal responses by providing a measure of ecological relevance to biological studies (Hofmann et al. 2011; Kapsenberg et al. 2017). Increasing our knowledge of the biological and physical drivers that regulate nearshore pH dynamics will help disentangle natural vs. human-caused pH variability.

The goal of this study was to capture high-frequency, interannual pH measurements at two nearshore sites in the Beaufort Sea that differ in their proximity to a major river system. Both sites lie within the Stefansson Sound Boulder Patch kelp community, which has been the focus of numerous biological and ecological investigations since its discovery in the 1970s (Bonsell and Dunton 2021). The occurrence of boulders and cobbles that support the only known kelp community in the Beaufort Sea, which lies at the mouth of a major river delta, has long been an enigma, both with respect to the rock substrata (whose mineralogy is foreign to Alaska) and the persistence of a rich epilithic flora and fauna in a depositional environment (Dunton et al. 1982). Different assemblages of kelp, macroalgae, crustose coralline algae, and epilithic invertebrates across Stefansson Sound (Muth et al. 2020; Bonsell and Dunton 2021) suggested that these distributional patterns (especially in crustose coralline algae) may be reflective of changing physicochemical conditions related to annual inflow freshwater events in the late spring from the Sag River.

Our data includes under-ice measurements, which are difficult to capture during the eight-month period of continuous ice cover. Spatial placement of sensors at two sites that vary in their proximity to the Sag River allowed for comparisons between areas of differing water masses (marine dominated vs. seasonal freshwater influenced). This seasonally dynamic region of the inner shelf and coast is an important foraging area for thousands of migrating waterfowl and many species of anadromous fish that are critical resources for native Inupiat subsistence hunters. Coastal areas of the Arctic are also undergoing rapid transformation in response to regional climatic warming. We measured pH, salinity, temperature, and total alkalinity from discrete water samples and estimate aragonite saturation levels to further understand water chemistry effects on both kelp and calcifying organisms in Stefansson Sound (*see* Muth et al. 2020, 2021). To our knowledge, this is the first continuous, high-frequency biennial time series of pH data from the Arctic Ocean.

Methods

Study sites and background

Sea-Bird (Satlantic) SeaFETs and SBE 37-SM MicroCATs C-T (P) were deployed July 2016–July 2018 at two sites within the Boulder Patch, Stefansson Sound, Alaska (Fig. 1). Site E-1 (70°18.8665 N, 147°44.0413 W; 4.5 m depth) lies within 3.5 km of the Sag River Delta where bottom water salinities are often < 20 by late June owing to inputs during the spring freshet (Bonsell and Dunton 2021). Site DS-11 (70°19.3248 N, 147°34.8816; 6 m depth) is centrally located in Stefansson Sound and is largely buffered against Sag River water owing to its proximity to the Beaufort Sea and ocean exchanges (corresponding salinities are always greater than 20; Bonsell and Dunton 2021). Sensors were embraced with Styrofoam collars attached to benthic weights and suspended in the water column (~1 m from the bottom), allowing the sensor to maintain an upright, yet flexible position to resist transport by deep-draft ice. Sensors deployed 4 August 2016 to 25 July (DS-11) and from 30 July (E-1) 2017, recorded values hourly (average of 20 samples per frame with one burst). The 2 August 2017 to 16 July 2018 deployments recorded values every 2 h to increase battery life for the year-long deployment (same settings as 2016 deployments).

Calibration and pH data processing

Water samples were collected via SCUBA by hand using a van Dorn water sampler proximate to each sensor at deployment and retrieval (temporally aligned with sensor sampling time at the top of the hour). Samples were immediately fixed with saturated HgCl₂ (75 μ L in 250 mL for pH and 37.5 μ L for 125 mL for A_T), and stored at 4°C until analysis (Dickson et al. 2007). Spectrophotometric pH was measured at 25°C for 2016 deployment samples and 20°C for 2017 retrieval and deployment samples using m-cresol purple sodium salt, dye content 90% (Sigma-Aldrich; spectrophotometric method, Dickson et al. 2007). An automated open-cell Gran titration system (ASALK2; Apollo SciTech) was used to measure total alkalinity (SOP 3b, Dickson et al. 2007). The in-situ temperature of the seawater samples was recorded using the SeaFET's thermistor. A single-point calibration method was used to calculate in situ pH_T (total hydrogen ion scale, CO₂Calc, Robbins et al. 2010) following Bresnahan et al. (2014) using constants from Mehrbach et al. (1973) refit by Dickson and Millero (1987). Water samples were collected at the

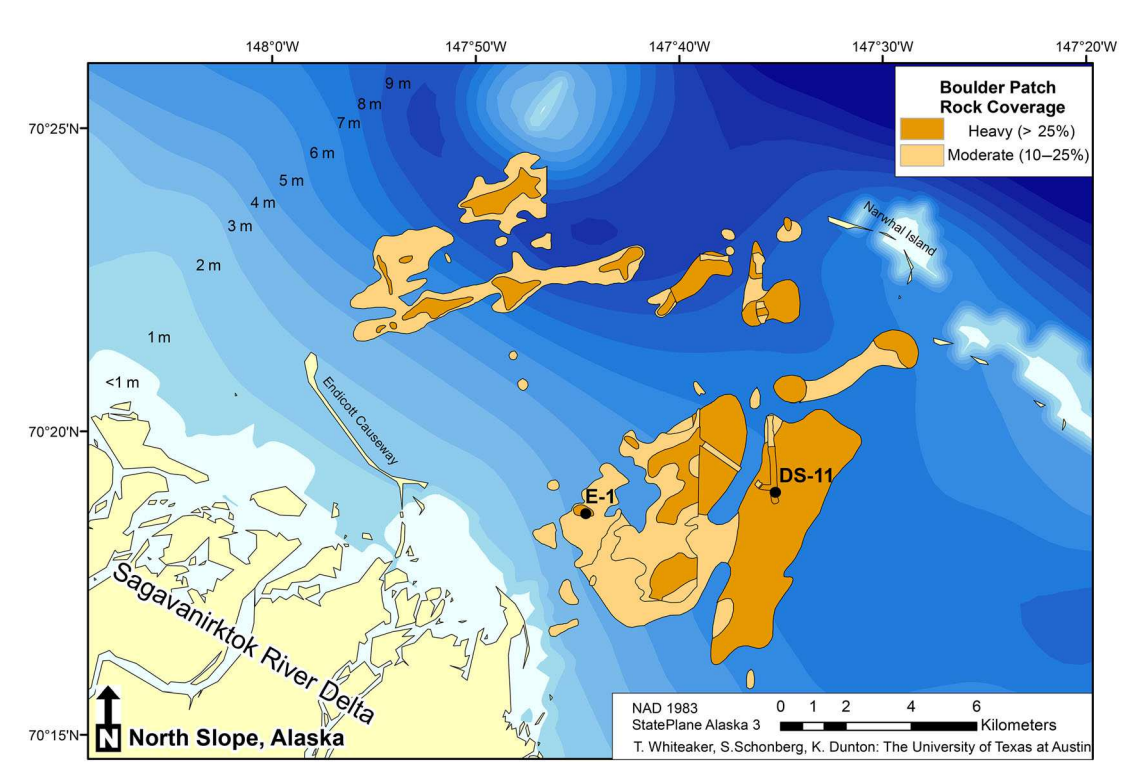


Fig. 1. The Stefansson Sound Boulder Patch and instrument deployment sites. E-1 (4.5 m; inshore) and DS-11 (6 m; offshore), differed in proximity to the Sagavanirktok River, creating different salinity and chemistry regimes (adapted from Bonsell and Dunton 2018).

time of deployment in 2016 because of field logistical constraints which did not allow for adequate conditioning of the electrodes. A post-retrieval visual inspection of the data clearly demonstrated a stabilization in pH values within ~ 48 h of deployment. Thus, a single-point calibration was applied 48 h from the time the water sample was initially collected, when pH stabilization had clearly taken place (Supporting Information Fig. S1). For the 2017 datasets, sensors were already conditioned at deployment and a single point calibration was applied at the time the water sample collection.

Aragonite saturation levels were calculated for each dataset using pH, salinity, and temperature values, and estimated total alkalinity from discrete water samples taken throughout the Boulder Patch in July 2018 (n=13; CO₂Calc, USGS). Total alkalinity was measured using the techniques described above and regressed against salinity values (y=31.032x+1653.3; $r^2=0.61$; Supporting Information Fig. S2). Temperature and salinity values were plotted against the freeze point line of seawater and any values that fell below the freeze point line were not included in the analysis as these values were not valid and due to sensor error (Supporting Information Fig. S3). All data are deposited and accessible on the Beaufort Lagoon Ecosystems Long-Term Ecological Research site (https://ble.lternet.edu/finddata).

Estimated pH uncertainty

During the 2016–2017 deployment, pH uncertainty was estimated for each time series by calculating the absolute value of

the difference between the reported calibrated SeaFET value and the laboratory measured in situ pH value of the reference sample taken prior to retrieval (Miller et al. 2018). Reference samples were not collected prior to instrument retrieval for the 2017-2018 deployment. Our total alkalinity and salinity measurements were collected independently from the bottle samples used to calibrate the pH time series. We used 13 pH (national bureau of standards; NBS) values collected at both sites over a wide range of salinities to regress alkalinity against salinity to constrain the range of pH values measured throughout the year. In order to estimate a conversion factor between pH_{NBS} and pH_{T} , spectrophotometric pH was measured at 25°C from a certified reference material (CRM, Dickson Laboratory, UC Scripps, Batch 171) that was diluted with deionized water to create five salinity samples (33.43, 20, 15, 10, 5). pH_T was calculated for the serial salinity dilution using spectrophotometric pH measured at 25°C, in conjunction with the A_T, temperature and salinity of each sample. A calibrated PRO DSS YSI sonde (same model used in original field measurements) was then used to measure pH_{NBS} for each salinity sample created. Although there is greater uncertainty associated with the data sonde (pH \pm 0.01), this calibration protocol allowed the use of the pH_{NBS} values to estimate sensor uncertainty ($pH_{NBS} + 0.118 = pH_T$; Supporting Information Table S1). As a result, uncertainty estimates for the 2017-2018 deployment period were characterized as the absolute difference between the converted pH_T value measured by the data sonde and the calibrated SeaFET value.

Table 1. Temperature, salinity, pH, dataset pH uncertainties, and Ω_{arag} levels for both sites and years. Mean values \pm standard error (SE).

| | E-1 | | DS-11 | |
|------------------------------------------|---------------------------|---------------------------|---------------------------|---------------------------|
| | August 2016– July 2017 | August 2017– July 2018 | August 2016– July 2017 | August 2017– July 2018 |
| pH range | 7.83–8.70 | 7.67–8.67 | 7.79–8.69 | 7.47–8.23 |
| Open water period pH average (SE) | 8.00 (>0.000) | 8.02 (>0.000) | 7.97 (0.001) | 7.65 (0.004) |
| Ice-covered period pH average (SE) | 7.95 (0.001) | 7.93 (0.001) | 7.92 (0.002) | 7.51 (0.006) |
| pH uncertainty | 7.97 - 7.99 = 0.02 | 8.24 - 8.16 = 0.08 | 7.84 - 7.93 = 0.09 | 7.51 - 7.54 = 0.03 |
| (sensor value – discrete water sample) | | | | |
| Temperature range (°C) | -1.87 to 7.08 | -1.86 to 9.73 | -1.88 to 6.08 | -1.91 to 9.05 |
| Salinity range | 19.07-34.35 | 0.01-34.02 | 21.93-34.51 | 22.78-34.86 |
| Ω_{arag} level range | 0.88-4.93 | 0.08-4.89 | 0.89-4.79 | 0.33–1.66 |

Statistics

All abiotic factors, pH, salinity, and temperature and calculated Ω_{arag} were analyzed by averaging each factor for each month of deployment for the 2016–2017 and 2017–2018 deployment periods for each site (four groups). Due to

unequal sample sizes and non-normal data distributions, the non-parametric statistical test Kruskal–Wallis was used to compare years and sites. Significant results were additionally followed by a Dunn test to use pairwise comparisons to determine what factor (site or year) was driving the significant

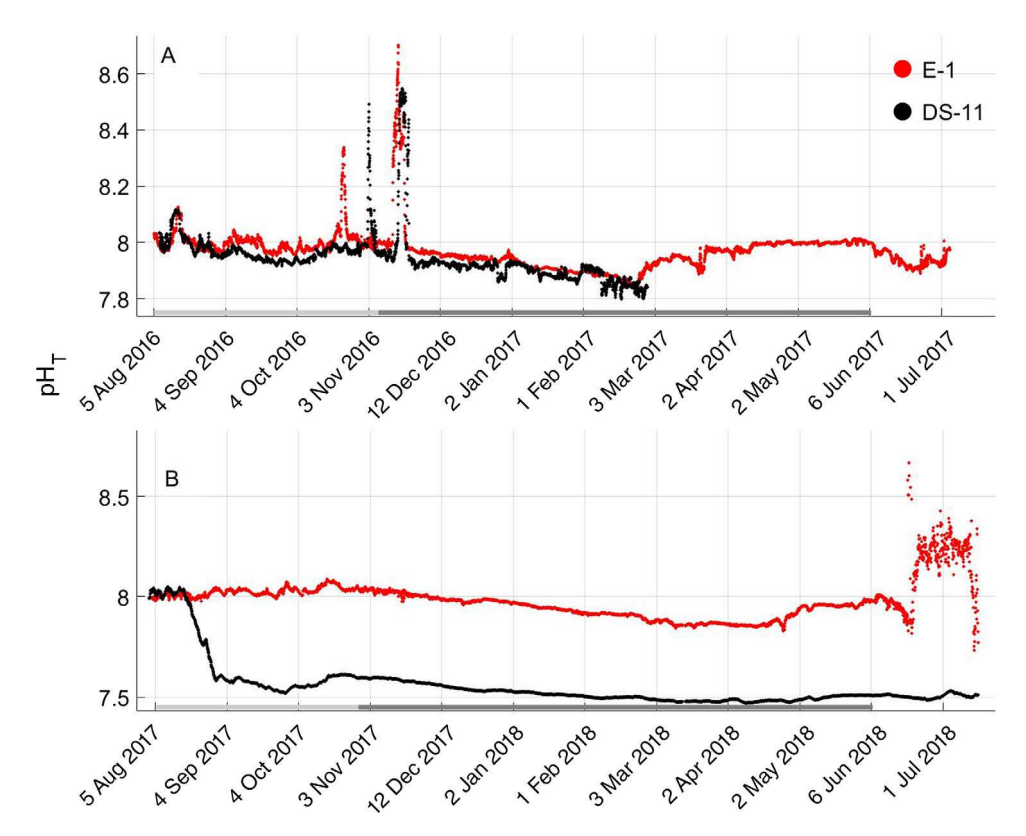


Fig. 2. Continuous pH_T values for sites DS-11 (black) and E-1 (red). (**A**) 2016–2017 deployment, (**B**) 2017–2018 deployment. *X*-axis bar shading represents the periods of open water (light gray), ice cover (dark gray), followed by post peak discharge of the Sagavanirktok River and ice break-up (no shading).

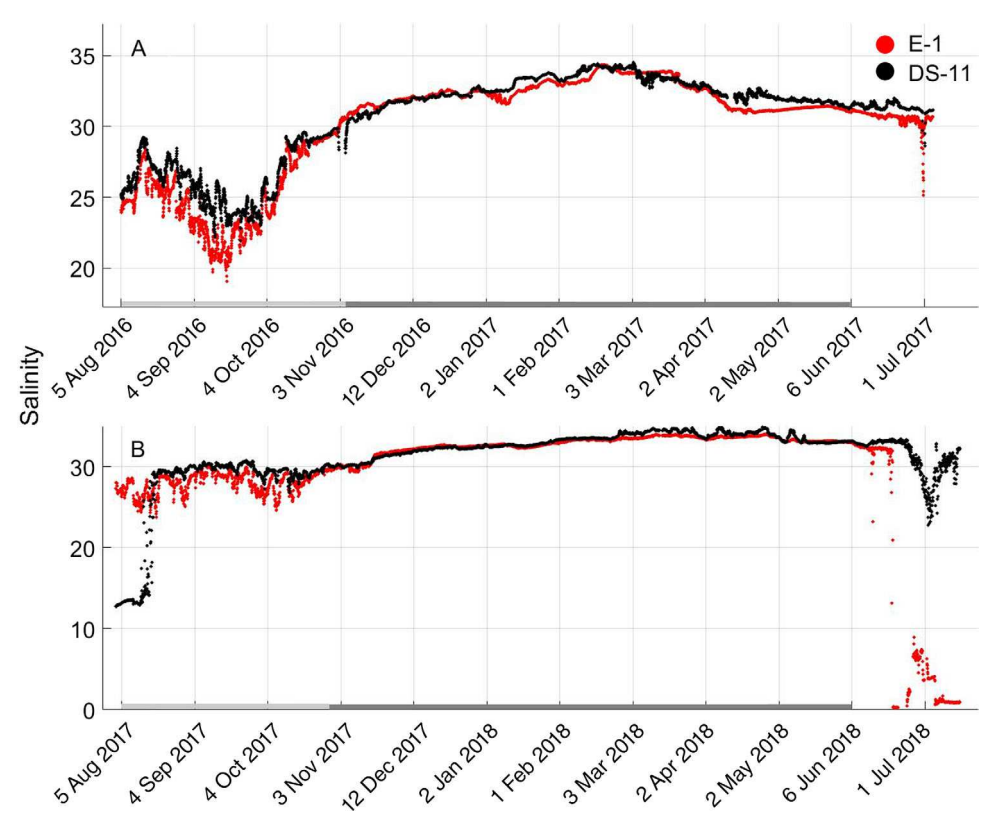


Fig. 3. Continuous salinity values for sites DS-11 (black) and E-1 (red). (A) 2016–2017 deployment; (B) 2017–2018 deployment. X-axis bar shading represents the periods of open water (light gray), ice cover (dark gray), followed by post peak discharge of the Sagavanirktok River and ice break-up (no shading).

differences in values. All statistics were run using R version 1.2.1335.

Results

We collected continuous pH data over two annual periods on the Beaufort Sea coast. These 12-month periods were characterized by a confluence of interacting factors including sea ice coverage, low water temperature, low total alkalinity river water, and intense seasonal and annual variability. Coastal ocean pH, salinity, and temperature followed seasonally distinct transitions that were related to four main events: summer open water, fall freeze-up, winter ice cover, and spring freshet. Freeze-up was defined as an icepack of nine-tenths or "very close pack" (Arctic Data Integration Portal, portal.aoos. org). Freeze-up was estimated to occur 4-6 of November in 2016 and 26-28 of October for 2017. Peak discharge of the Sag River predictably occurs in late May and early June (McClelland et al. 2014).

pH time series

For the 2016–2017 deployment, pH values varied ~ 0.87 pH units at E-1, and ~ 0.9 pH units at DS-11 (Table 1). pH values fluctuated little following instrument deployment in early

August, but anomalous spikes in fall 2016 were likely associated with changes in the physicochemical environment with the freezing of coastal waters (Fig. 2A), as freeze-up dates corresponded to increases in pH. Both sites showed a slight decrease in pH from November 2016 through February 2017 and subtle increases in pH were observed from March until break-up at E-1; Fig. 2A). Unfortunately, the SeaFET at DS-11 lost power on 28 February 2017 and at E-1 on 4 July 2017. Clear shifts in average pH values were seen between ice-covered and open water regimes; pH was generally lower during the ice-covered period (Table 1). DS-11 averaged 7.97 (± 0.001) during months of open water and 7.92 (± 0.002) when ice was present. E-1 values were 8.00 (± 0.000) during the open water period and 7.95 (± 0.001) under the ice.

The August 2017–July 2018 deployment revealed annual variation in pH values of ~ 1 pH unit at E-1 and ~ 0.76 at DS-11 (Table 1). Two weeks after instrument deployment, a distinct drop in pH from ~ 8 to ~ 7.6 began in mid-August at offshore site DS-11 (Fig. 2B). Following ice formation in late October, pH continued to decrease at DS-11 until the spring freshet in May. In contrast to the August 2016–July 2017 data, much lower pH values were recorded at DS-11 during the 2017–2018 ice-covered period. The anomalous pH spikes in the fall of 2016 at both sites (Fig. 2A) were not seen in 2017

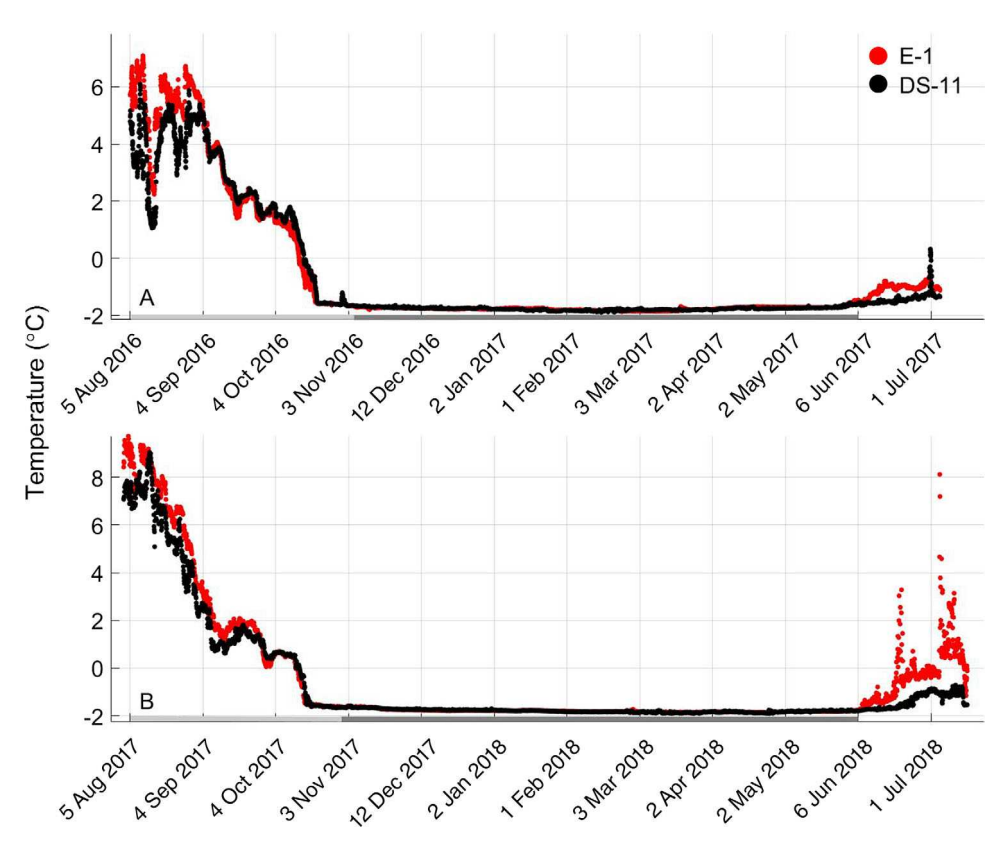


Fig. 4. Continuous temperature values for sites DS-11 (black) and E-1 (red). (**A**) 2016–2017 deployment, (**B**) 2017–2018 deployment. *X*-axis bar shading represents the periods of open water (light gray), ice cover (dark gray), followed by post peak discharge of the Sagavanirktok River and ice break-up (no shading).

(Fig. 2B). On 18 June 2018, the freshwater input signal from break-up at inshore site E-1 was coincident with a substantial increase in pH and a steep drop in salinity from 32 to near zero (Figs. 2B, 3B), but the drop in salinity at DS-11 in early July (32–22), was insufficient to trigger a pH change. Like 2016–2017, under-ice pH for 2017–2018 values were lower than open water averages, and pH values differed between periods of open water, and ice-cover, and break-up for each site (Table 1). Results from a Kruskal–Wallis test indicated significant differences of pH among site/year groups (Kruskal–Wallis $\chi_{2,3}=12.54$, p-value = 0.01). Post hoc pairwise comparisons showed that mean pH values at DS-11 (2016–2017) and E-1 were significantly different than the mean pH value at DS-11 in 2017–2018 (p<0.001; Supporting Information Fig. S4).

Estimated pH uncertainty

Estimated uncertainty for the August 2016–July 2017 deployment was 0.042 for E-1 and 0.046 for DS-11, respectively. August 2017–July 2018 uncertainty values were 0.085 for E-1 and 0.028 for DS-11 (Table 1). The higher uncertainty values for E-1 in the second year could be attributed to our use of a data sonde to measure pH. However, we applied the same methods described above to convert pH_{NBS} to pH_T for DS-11

and obtained a (0.028) uncertainty value. Conditions at DS-11 were much more stable at the time of retrieval and this may have affected anomaly calculations (Fig. 2B).

Temperature and salinity time series

Ranges in temperature (E-1: 8.95° C; DS-11: 7.96° C) and salinity (E-1: 15.28; DS-11: 12.58) were similar between sites in 2016–2017 (Figs. 3 and 4, Table 1). However, in 2017–2018, salinities differed drastically between sites during peak freshwater discharge (temperature range E-1: 11.59° C; DS-11: 10.96° C; salinity range E-1:34.01; DS-11: 12.08; Figs. 3 and 4; Table 1). These patterns illustrate the dynamic conditions of this nearshore estuarine environment but also highlight the need for long-term monitoring. We found no significant differences between mean salinity values for sites and years because of the naturally high variance that is characteristic of estuarine systems (temperature: Kruskal–Wallis $\chi_{2,3}=0.75894$, p-value = 0.8593; salinity: Kruskal–Wallis $\chi_{2,3}=1.2105_3$, p-value = 0.7505; Supporting Information Fig. S4).

Influence of salinity on pH

The Sag River had a significant effect on water composition and chemistry at both sites. Salinity and pH exhibited marked relationships that highlighted the seasonal influence of

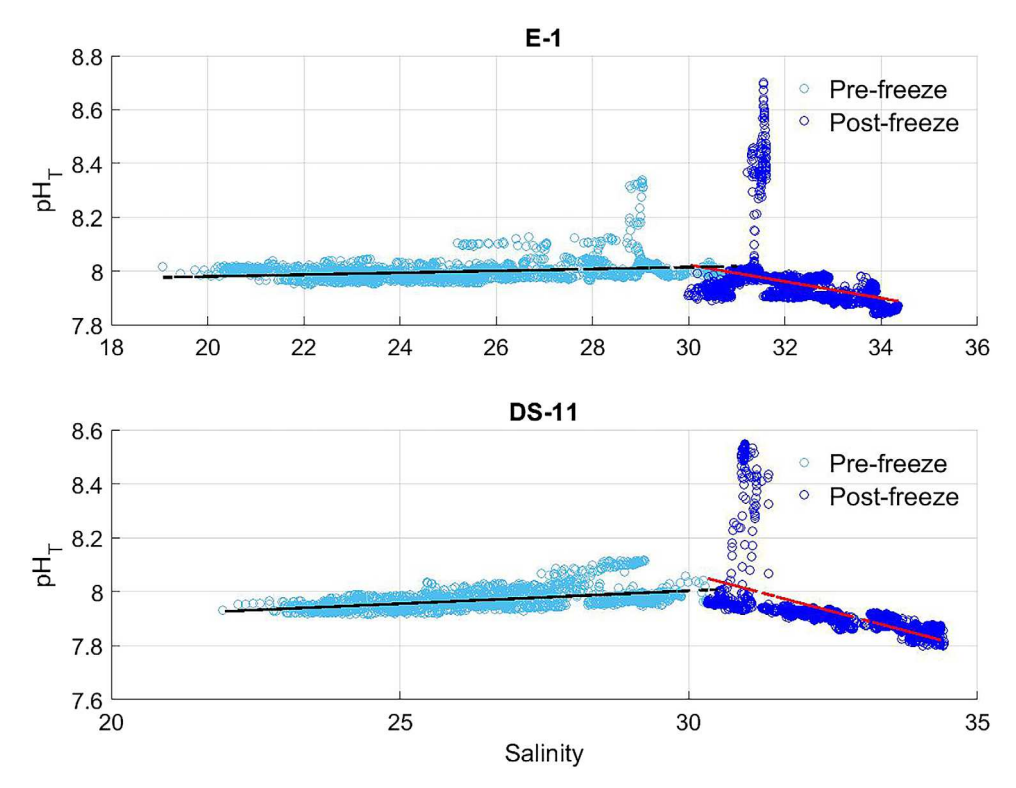


Fig. 5. Salinity vs. pH_T relationships for 2016–2017 deployments separated by open water (pre-freeze; light blue circles) and ice cover (post-freeze; dark blue circles) time frames. Freeze-up was estimated to occur on 4–6 November 2016 at both sites (**A**) E-1 and (**B**) DS-11. Dotted lines represent general trendlines of the pre-freeze (open water) and post-freeze (ice cover) salinity and pH relationships.

freshwater input into these coastal systems. Annually, distinct salinity and pH relationships were visible before and after freeze-up for both sites (Figs. 5 and 6). These relationship regime shifts were seen in both deployment years and signaled a change between ice covered stabilized ocean water and ocean water mixed with freshwater from the Sag River. Generally, the relationship showed lower pH_T and higher salinity values after freeze-up and higher pH with lower salinity levels prior to freeze-up (Figs. 5 and 6). The inverse relationship between pH and salinity (high pH associated with lower salinity values) was also visible during break-up at E-1 in 2018, where low salinity values (near 0) were associated with an increase in pH (Fig. 2B).

Estimated Ω_{arag} time series

Estimated aragonite saturation levels ranged from 0.88 to 4.93 at E-1 and 0.89 to 4.79 at DS-11 for the 2016–2017 deployment, with values near equilibrium (Fig. 7A; Table 1) for much of the ice-covered period at both sites. Peaks in aragonite saturation levels corresponded to peaks in pH (Fig. 2). The 2017–2018 dataset exhibited greater aragonite saturation variability between sites than 2016–2017 (Fig. 7B) and this was also reflected in other parameters (see Figs. 2–4; Table 1). E-1 2017–2018 aragonite saturation fluctuated from 0.08 to 4.89 and 0.33 to 1.66 at E-1. Lowest values for both sites were

reached during the spring freshet in July 2018. Annual mean levels compared between sites and years were significantly different (Kruskal–Wallis $\chi_3^2=18.4929$, p-value = 0.00). Post hoc pairwise comparisons show that the DS-11 2017–2018 deployment was significantly different than all other site and year deployments (Supporting Information Fig. S4). We found that low aragonite saturation (associated with periods of high pH) corresponded with low salinity and total alkalinity, highlighting the critical role that salinity and associated total alkalinity values play in carbonate chemistry that is independent of pH.

Discussion

Nearshore pH, total alkalinity and other carbonate chemistry parameters have been reported for the Arctic Ocean (Mathis et al. 2011), but the data reported here are the first to include multi-year, continuous measurements in the shallow (< 6 m) nearshore environment. Our measurements show the relatively large comparative spatial effect of a major freshwater source on pH as driven by salinity. Depth and location within pycnocline stratification layers can lead to values that may not represent the water column in offshore deeper environments (Miller et al. 2019). Measurements often include only surface waters that are heavily influenced by atmospheric exchange and varying freshwater sources (e.g., river run-off or

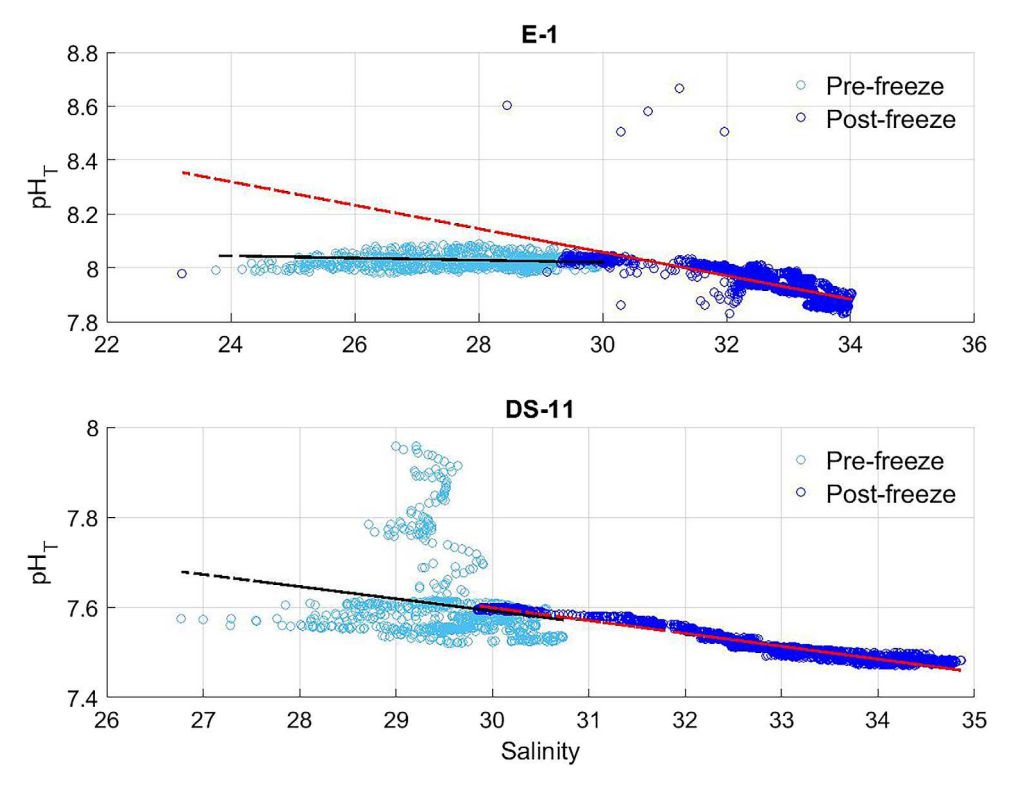


Fig. 6. Salinity vs. pH_T relationships for 2017–2018 deployments separated by open water (pre-freeze; light blue circles) and ice cover (post-freeze; dark blue circles) time frames. Freeze-up was estimated to occur 26–28 October 2017 at both E-1 and DS-11. Dotted lines represent general trendlines of the pre-freeze (open water) and post-freeze (ice cover) salinity and pH relationships. Note the trendline for post-freeze at E-1 continues past the grouping of data points due to one data point near a salinity of 23 and pH of 8.

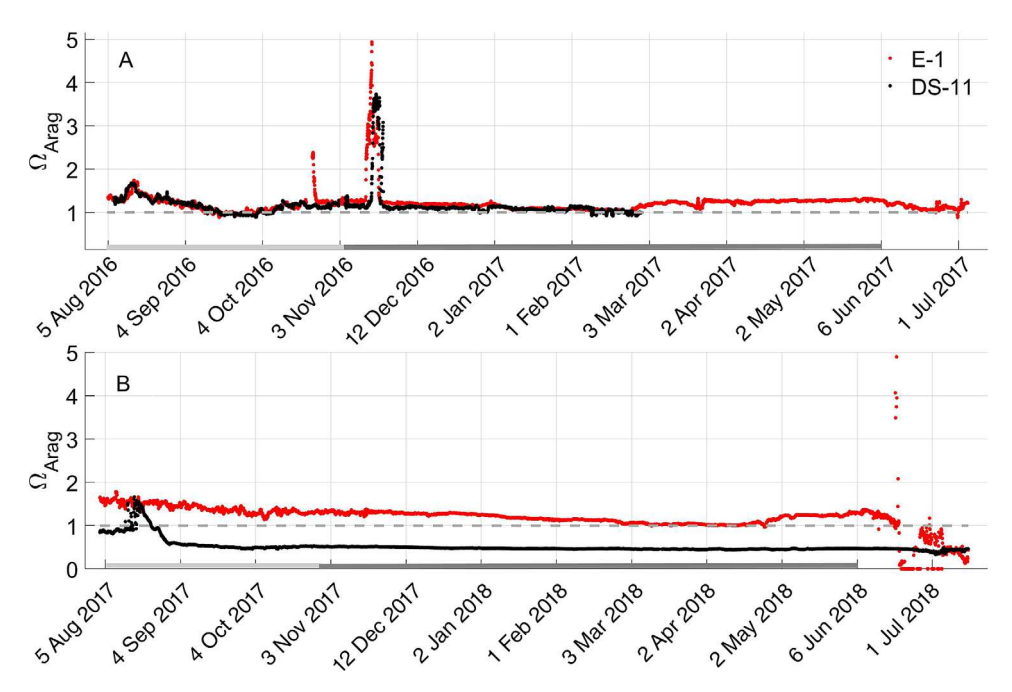
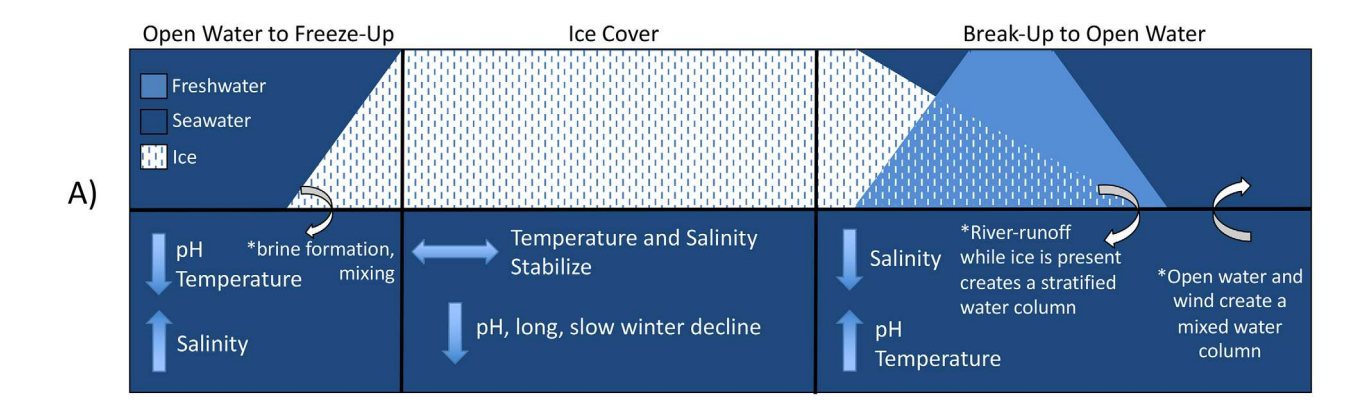


Fig. 7. Aragonite saturation levels for E-1 (red) and DS-11 (black) for 2016–2017 (**A**) and 2017–2018 (**B**). The dotted line represents equilibrium with respect to aragonite. Values less than one favor dissolution while values above the line favor precipitation of aragonite. X-axis bar shading represents open water (light gray), ice covered (dark gray), and post break-up open water (no shading).



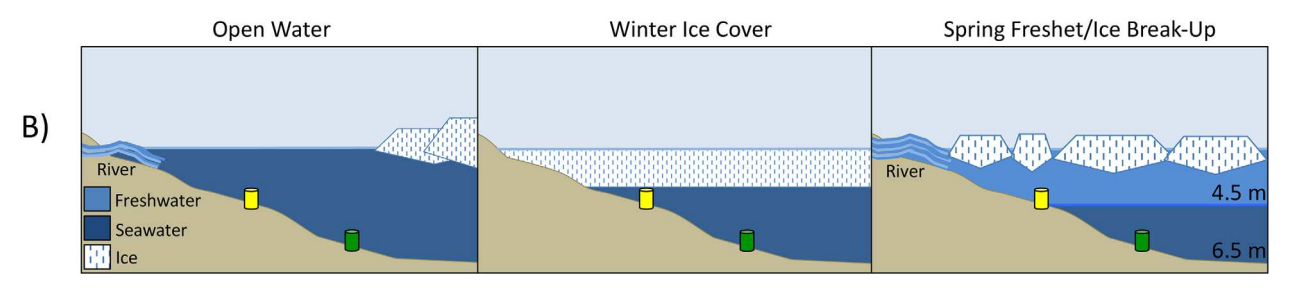


Fig. 8. (**A**) Generalized seasonal changes of abiotic factors (temperature, salinity, pH) as ocean conditions transition from open water to freeze-up, ice cover, ice break-up (punctuated by the spring freshet), and back to open water conditions. The shapes of the polygons in (**A**) represent the ramping up and down of ice cover and freshwater run-off, respectively. Biological processes (e.g., respiration) are likely responsible for the slow winter decline in pH during ice-covered months, although other physio-chemical processes may alter pH values. (**B**) Seasonal patterns of water column stratification in relation to depth of the site and sensor (E-1, yellow; DS-11, green).

ice melt; Yamamoto-Kawai et al. 2009; Tank et al. 2012). Our data captured conditions near the seabed and are representative of the water that is affecting the epilithic assemblages of the Arctic, near-shore benthic communities. These data also highlight the importance of understanding how freshwater sources can affect ocean carbonate chemistry on regional scales.

General seasonal patterns

Seasonal variability in pH, temperature and salinity corresponded to distinct time periods associated with open water, freeze-up, ice cover, and the spring freshet (Figs. 2–4, 8). These distinct seasonal separations have been reported previously (Weingartner et al. 2017), and our results corroborate the patterns reported, albeit in higher frequency. In general, as near-shore waters transition from open water to ice cover with the onset of freezing temperatures and shorter days, salinity levels increase, and water temperature and pH values decrease (Fig. 8). Following ice formation, pH values continue to decrease slowly until light begins to penetrate the ice cover in early spring with increasing daylength and solar inclination. The initial decrease in pH may be driven by sediment respiration and water column heterotrophy that produces high pCO_2 levels. However, ice formation alone has been shown to

increase pCO_2 in the absence of biological processes (DeGrandpre et al. 2019). In spring, the large pulse of freshwater runoff often creates a stratified water column in June, which in shallower inshore areas can result in freshwater conditions that can extend completely to the bottom for several days (as occurred at E-1 in 2018). In deeper offshore areas, wind can facilitate mixing as ice retreats, sometimes causing moderate drops in salinity before the onset of full open water conditions and a well-mixed water column.

In contrast to other nearshore polar ecosystems, we did not observe a sudden increase in pH that typically signals the onset of seasonal primary productivity in early summer. In the nearshore Antarctic, a rapid increase in pH at the beginning of the austral summer results from phytoplankton blooms that increase pH by 0.3–0.4 units compared to stable wintertime values (Hofmann et al. 2015). While a small increase in pH appears during the transition from spring to summer at E-1 in both years, this pattern was not observed at DS-11 in 2018. One potential cause for the lack of a pH increase at DS-11 in 2018 may be related to low light levels caused by highly turbid water as sediment-laden sea ice melts in Stefansson sound between mid-June and mid-July (Bonsell and Dunton 2018). Benthic light levels at DS-11 averaged only 0.142 μ mol photons m² s⁻¹ \pm 0.021 from 15 June through

15 July 2018 (Dunton and Bonsell 2020). The prolonged presence of ice within the sound in 2018 also likely dampened any primary production pulse and subsequent increase in pH.

Annual variations and anomalies

Despite seasonal and annual patterns seen over the 2-vr deployment, annual and spatial variations occurred between sites and years. In 2016, pH increases were observed at E-1 and DS-11 (Fig. 2B) during freeze-up in the fall. The reason for these pH increases is not clear. It is highly unlikely that amplitude anomalies were driven by an increase in primary production, since the fall period is characterized by a turbid water column, which combined with low sun angles, produce very low irradiance levels (October through November 2016 averages; E-1 0.059 µmol photons m² s⁻¹ \pm 0.011, DS-11 0.039 μ mol photons m² s⁻¹ \pm 0.006; Dunton and Bonsell 2020). Since increased pH levels were observed at both sites around the same period as freezeup, the higher values could be a result of brine formation and water column turnover that disturbs the bottom and increases turbidity. Weingartner et al. (2017) also reported that conductivity sensors fail during this time period and speculated that increases in turbidity obstructed the sensors. A similar pH anomaly was seen in the Canadian Arctic within days of freeze-up, and the sudden increase in pH was attributed to increases in total alkalinity and dissolved inorganic carbon in conjunction with thermochemical reactions from temperature changes (Duke 2019).

The 2017–2018 pH dataset exhibited different patterns than in 2016-2017 at both sites. The pH anomalies that occurred during freeze-up in fall 2016 did not occur in fall 2017; pH also increased dramatically at E-1 in association with the June freshwater pulse from the Sag River. At DS-11, a dramatic decrease in pH from ~ 8.0 to 7.6 occurred mid-August 2017 (Fig. 2B). The lack of continuous baseline data in the nearshore Arctic creates difficulties in discerning a possible sensor error for the low pH values at DS-11, but the DS-11 2017-2018 uncertainty was one of the lowest (0.03) of all datasets (Table 1). In addition, pH data from Kaktovik Lagoon, located 150 km east of Stefansson Sound in the Beaufort Sea, acquired in summer 2018-2019 (Miller et al. 2021) showed a similar pattern; pH dropped from 8.3 to 7.7 over a 2-wk period in fall 2018 and continued to slowly decrease to 7.6 through the ice-covered period as noted at DS-11 through spring 2018. For these reasons, we cannot assume that the deviation in the pH time series for DS-11 in Stefansson Sound is a product of sensor malfunction.

The decreasing trend in pH values during the transition from the late summer open water period through the period of ice cover could be the result of shallow, ice-covered waters dominated by heterotrophy. Partial pressure of CO₂ values increase with respiration since the ice creates a closed system with no atmospheric mixing. We have no evidence that the occurrence of distinct water masses with distinct pH characteristics were responsible for observed differences spatially or

temporally (Supporting Information Fig. S5). Instead, the marked difference during the 2017-2018 deployment was constrained by each site's distance from the Sag River, where the strong drop in salinity at E-1 in June 2018 was temporally synced with an increase in river discharge. The depth of the pycnocline, which we were unable to measure during breakup, likely played a role in how each site was influenced by changes in salinity. The shallower site (E-1; ~4.5 m) has a higher potential for the benthos to become completely exposed to freshwater (as seen in 2017-2018) during the spring freshet, while the deeper site (DS-11; ~6 m) is more likely buffered by marine waters. These exposure discrepancies can be seen in the distribution of crustose coralline algae within the Boulder Patch (Muth et al. 2020). Benthic zones exposed to freshwater are devoid of crustose coralline algae that are not able to persist in the carbonate chemistry regimes created by input from the Sag River.

There was a distinct temporal separation in the relationship between salinity and pH that occurred before and after freeze-up from both sites in 2016–2017 (Fig. 5). Separations were seen in 2017 as well, although the not as distinct as in fall 2016 (Fig. 6). In general, pH increased as freshwater from the Sag River increased (Fig. 2, lower panel). Although a number of processes (wind, storms, freeze-up, break-up, and freshwater pulses) can drive these water mass changes, the separations likely represent a shift from a period of run-off from the Sag River to a stable, ice-covered period dominated by polar marine layer waters (lower salinity, higher pH vs. higher salinity, lower pH) that are continually upwelled and transported onto the inner shelf under the ice.

Seasonal variability of the nearshore Arctic creates carbonate chemistry regimes that are unique and ephemeral, spatially and temporally. Although salinity levels dropped with freshwater input at our inshore site, pH levels increased due to the alkaline nature of the freshwater source. The Sag River is classified as a mountain stream (Craig and McCart 1975), which drains limestone deposits and discharges alkaline freshwater into Stefansson Sound. Arctic river alkalinities are increasing with changes in precipitation, permafrost depth, groundwater flow, and vegetation coverage (Drake et al. 2018), and our data illustrate the connectivity of this riverine input with the Arctic nearshore system. Other sources of freshwater, such as sea ice melt, are much lower in total alkalinity ($\sim 300 \, \mu \text{mol kg}^{-1}$; Yamamoto-kawai and Tanaka 2005) and aragonite saturation levels of the resultant mixed ocean water is decreased compared to alkaline freshwater sources, such as the Sag River. However, most freshwater sources (e.g., ice melt, precipitation, river discharge) combined with ocean water will reduce Ω_{arag} in these nearshore systems, negatively affecting calcifying organisms inhabiting these mixed water zones.

Estimated aragonite saturation levels time series

Aragonite saturation levels calculated from the nearshore Arctic dataset reveal values less than 1.5 at both the inshore

and offshore sites that remained relatively constant under the ice (Fig. 7). Similar aragonite saturation level ranges were reported for the Antarctic but increases in pCO₂ and subsequent decreases in pH drive lower aragonite saturation levels while total alkalinity values remain constant (Kapsenberg et al. 2017). Similar trends were seen in Ischia, Italy when large increases in pCO_2 caused lower $\Omega_{calcite}$ (Kroeker et al. 2013). In contrast, our aragonite saturation levels decreased when total alkalinity levels dropped with freshwater input from the Sag River (Figs. 4–6). Our values were based on measured total alkalinity values (see Supporting Information Fig. S2). Ideally, continuous pCO_2 or total alkalinity values would have been collected with pH, temperature, and salinity to calculate aragonite saturation levels, but this was beyond our capabilities at the time of deployment. Biological processes (CO₂ production) may have driven low aragonite saturation levels at the offshore site (DS-11) for the 2017-2018 deployment, as well as ice formation leading to increased pCO₂ and decreased pH values (DeGrandpre et al. 2019; Fig. 2B). Low aragonite saturation levels were not observed during the winter months of 2017-2018 at inshore site E-1, but profound decreases in aragonite saturation levels were seen during the freshet (Fig. 7B). The nearshore Arctic region's susceptibility to ocean acidification and low aragonite saturation levels are amplified by the additional alterations from freshwater influence (low total alkalinity) and the biological processes that create naturally lower ocean pH waters. It is important to note that CO₂Calc does not consider calcium within freshwater sources in the calculation of aragonite saturation levels.

The concentration of dissolved calcium in the Sag River is almost twice as high as other nearby Arctic rivers (Rember and Trefry 2004). Average calcium values for the Sag River are 24.48 mg L $^{-1}$, compared to the lower Kuparuk (10.43 mg L $^{-1}$) and the Colville (13.67 mg L $^{-1}$) as noted by McClelland et al. (2007), but still much lower than ocean Ca values (~ 400 mg L $^{-1}$; Perry et al. 2001). Aragonite saturation levels may be underestimated, especially during times of high amounts of freshwater influence (i.e., the freshet). Decreased salinity and total alkalinity values during break-up result in aragonite saturation levels below equilibrium (Fig. 7), causing significant stress to biota that possess calcium carbonate skeletons. Such events occur despite relatively high pH (values > 8.2), which may be common in nearshore waters of the Arctic in response to alkaline river drainage.

Projections for a rapidly warming Arctic include increased river discharge (Peterson et al. 2002) are likely to only exacerbate the effects of decreased salinity and total alkalinity values. In the Boulder Patch kelp community, crustose coralline algae and kelp are co-occurring foundation species that are strongly sensitive to lower aragonite saturation levels and salinity, respectively (Muth et al. 2020, 2021). The codependency of both species on each other is responsible for maintenance of the most diverse benthic assemblages on the

inner shelf of the Beaufort Sea (Dunton et al. 1982; Bonsell and Dunton 2021). Loss of either species results in lower diversity with the change in habitat structure. One of the most abundant groups in the shallow nearshore waters are mollusks, which are important food source that help supports a vibrant coastal fishery (von Biela et al. 2013) and thousands of wading and diving migrant seabirds (Brown 2006). The decrease or loss of biota that secrete calcium carbonate skeletons would have strong cascading trophic effects on upper-level trophic biota, especially those that are important for native subsistence hunters and fishers that inhabit Arctic coasts (Dunton et al. 2012).

Conclusions

We documented annual pH ranges of 1.0 pH units at the inshore site (E-1) in 2017-2018, a variation much larger than recorded in the Antarctic (0.40 and 0.42; Kapsenberg et al. 2017). Lower latitude locations tend to have less pH variation (Hofmann et al. 2011; Kapsenberg et al. 2017), but with some exceptions (up to 1.4; Hofmann et al. 2011). Biologically driven pH dynamics are common in temperate kelp forests and coral reefs where primary production is relatively high (Hofmann et al. 2011). Environments seasonally covered in ice experience biologically driven pH changes resulting from respiration (Matson et al. 2014), atmospheric exchange during subsequent open water periods (Sievers et al. 2015), and if near a freshwater source, decreases in both salinity and total alkalinity during the spring (Yamamoto-Kawai et al. 2009). Such events are invariably linked to ocean pH and carbonate chemistry, creating very dynamic systems with seasonal and annual variability.

Nearshore Arctic environments harbor highly productive communities (see Wilce and Dunton 2014 for benthic macroalgae) that are critical for maintaining ecologically important species that support subsistence lifestyles (Dunton and Schell 1987; Dunton et al. 2012). Our data provides the setting for the evaluation of future changes in the carbonate chemistry of nearshore Arctic systems and highlights the importance of daily, interannual and decadal variability in deciphering the complex relationships between salinity, temperature, and pH. The adaptations acquired by benthic species in the nearshore Arctic that allow them to tolerate large seasonal and annual variations in salinity and pH are not fully understood. They persist in environmental regimes (namely low pH and salinity) that would be detrimental to lower latitude marine species and are important for our understanding of ecosystem resilience in a changing climate.

Data availability statement

All data are deposited and accessible on the Beaufort Lagoon Ecosystems Long-Term Ecological Research site (https://ble.lternet.edu/finddata).

References

- Bates, N. R., J. T. Mathis, and L. W. Cooper. 2009. Ocean acidification and biologically induced seasonality of carbonate mineral saturation states in the western Arctic Ocean. J. Geophys. Res. Oceans **114**: 1–21. doi:10.1029/2008JC004862
- Bates, N. R., R. Garley, K. E. Frey, K. L. Shake, and J. T. Mathis. 2014. Sea-ice melt CO_2 -carbonate chemistry in the western Arctic Ocean: Meltwater contributions to air-sea CO_2 gas exchange, mixed-layer properties and rates of net community production under sea ice. Biogeosciences **11**: 6769–6789. doi:10.5194/bg-11-6769-2014
- Bonsell, C., and K. H. Dunton. 2018. Long-term patterns of benthic irradiance and kelp production in the central Beaufort sea reveal implications of warming for Arctic inner shelves. Prog. Oceanogr. **162**(February: 160–170. doi: 10.1016/j.pocean.2018.02.016
- Bonsell, C., and K. H. Dunton. 2021. Slow community development enhances abiotic limitation of benthic community structure in a high Arctic kelp bed. Front. Mar. Sci. **8** (February: 1–17. doi:10.3389/fmars.2021.592295
- Bresnahan, P. J., T. R. Martz, Y. Takeshita, K. S. Johnson, and M. LaShomb. 2014. Best practices for autonomous measurement of seawater pH with the Honeywell Durafet. Methods Oceanogr. **9**(October: 44–60. doi:10.1016/j. mio.2014.08.003
- Brown, S. C. 2006. Arctic wings: Birds of the Arctic national wildlife refuge. Manomet Center for Conservation Sciences.
- Büdenbender, J., U. Riebesell, and A. Form. 2011. Calcification of the Arctic coralline red algae Lithothamnion glaciale in response to elevated CO₂. Mar. Ecol. Prog. Ser. **441**: 79–87. doi:10.3354/meps09405
- Carstensen, J., and C. M. Duarte. 2019. Drivers of pH variability in coastal ecosystems [review-article]. Environ. Sci. Tech. **53**: 4020–4029. doi:10.1021/acs.est.8b03655
- Chierici, M., and A. Fransson. 2009. Calcium carbonate saturation in the surface water of the Arctic Ocean: Undersaturation in freshwater influenced shelves. Biogeosciences **6**: 4963–4991. doi:10.5194/bgd-6-4963-2009
- Cooper, L. W., J. W. McClelland, R. M. Holmes, P. A. Raymond, J. J. Gibson, C. K. Guay, and B. J. Peterson. 2008. Flow-weighted values of runoff tracers (δ^{18} O, DOC, Ba, alkalinity) from the six largest Arctic rivers. Geophys. Res. Lett. **35**: 3–7. doi:10.1029/2008GL035007
- Craig, P. C., and P. J. McCart. 1975. Classification of stream types in Beaufort Sea drainages between Prudhoe Bay, Alaska, and the Mackenzie Delta, N. W. T., Canada. Arctic Alpine Res. **7**: 183–198.
- DeGrandpre, M. D., C. Z. Lai, M. L. Timmermans, R. A. Krishfield, A. Proshutinsky, and D. Torres. 2019. Inorganic carbon and pCO₂ variability during ice formation in the Beaufort Gyre of the Canada basin. J. Geophys. Res. Oceans **124**: 4017–4028. doi:10.1029/2019JC015109

- Diaz-Pulido, G., K. R. N. Anthony, D. I. Kline, S. Dove, and O. Hoegh-Guldberg. 2012. Interactions between ocean acidification and warming on the mortality and dissolution of coralline algae. J. Phycol. **48**: 32–39. doi:10.1111/j.1529-8817.2011.01084.x
- Dickson, A. G., and F. J. Millero. 1987. A comparison of the equilibrium constants for the dissociation of carbonic acid in seawater media. Deep Sea Res. Part A Oceanogr. Res. Pap. **34**: 1733–1743. doi:10.1016/0198-0149(87) 90021-5
- Dickson, A. G., C. L. Sabine, and J. R. Christian. 2007. Guide to best practices for ocean CO₂ Measurements Report 8, pages 1–196.
- Drake, T. W., S. E. Tank, A. V. Zhulidov, R. M. Holmes, T. Gurtovaya, and R. G. M. Spencer. 2018. Increasing alkalinity export from large Russian Arctic Rivers. Environ. Sci. Tech. **52**: 8302–8308. doi:10.1021/acs.est.8b01051
- Duke, P. J. 2019. Describing seasonal marine carbon system processes in Cambridge Bay Nunavut using an innovative sensor platform. doi:10.11575/PRISM/36430
- Dunton, K., and C. Bonsell. 2020. Water column physiochemical measurements in the Boulder Patch, Beaufort Sea, Alaska, 1986–2018. urn:node:ARCTIC. doi:10.18739/A2P26Q457
- Dunton, K. H., E. R. K. Reimnitz, and S. Schonberg. 1982. An Arctic kelp community in the Alaskan Beaufort Sea. Arctic **35**: 465–484. doi:10.14430/arctic2355
- Dunton, K. H., and D. M. Schell. 1987. Dependence of consumers on macroalgal (*Laminaria solidungula*) carbon in an arctic kelp community: 813C evidence. Mar. Biol. **93**: 615–625. doi:10.1007/BF00392799
- Dunton, K. H., S. V. Schonberg, and L. W. Cooper. 2012. Food web structure of the Alaskan nearshore shelf and estuarine lagoons of the Beaufort Sea. Estuar. Coasts **35**: 416–435. doi:10.1007/s12237-012-9475-1
- Evans, W., J. T. Mathis, and J. N. Cross. 2014. Calcium carbonate corrosivity in an Alaskan inland sea. Biogeosciences **11**: 365–379. doi:10.5194/bg-11-365-2014
- Fabry, V. J., J. B. McClintok, J. T. Mathis, and J. M. Grebmeier. 2009. Ocean acidification at high latitudes: The bellwether. Oceanography **22**: 160–171.
- Gangstø, R., M. Gehlen, B. Schneider, L. Bopp, O. Aumont, and F. Joos. 2008. Modeling the marine aragonite cycle: Changes under rising carbon dioxide and its role in shallow water CaCO₃ dissolution. Biogeosciences **5**: 1057–1072. doi:10.5194/bg-5-1057-2008
- Hofmann, G. E., and others. 2011. High-frequency dynamics of ocean pH: A multi-ecosystem comparison. PLoS One **6**: e28983. doi:10.1371/journal.pone.0028983
- Hofmann, G., A. L. Kelley, E. C. Shaw, T. R. Martz, and G. E. Hofmann. 2015. Near-shore Antarctic pH variability has implications for the design of ocean acidification experiments. Sci. Rep. 5: 1–10. doi:10.1038/srep09638

- Kapsenberg, L., S. Alliouane, F. Gazeau, L. Mousseau, and J. P. Gattuso. 2017. Coastal ocean acidification and increasing total alkalinity in the northwestern Mediterranean Sea to cite this version. Ocean Sci. Eur. Geosci. Union **13**: 411–426. doi:10.5194/os-13-411-2017
- Kelley, A. L., and J. J. Lunden. 2017. Meta-analysis identifies metabolic sensitivities to ocean acidification. AIMS Environ. Sci. 4: 709–729. doi:10.3934/environsci.2017.5.709
- Kroeker, K. J., R. L. Kordas, R. N. Crim, and G. G. Singh. 2010. Meta-analysis reveals negative yet variable effects of ocean acidification on marine organisms. Ecol. Lett. **13**: 1419–1434. doi:10.1111/j.1461-0248.2010.01518.x
- Kroeker, K. J., M. C. Gambi, and F. Micheli. 2013. Community dynamics and ecosystem simplification in a high-CO₂ ocean. Proc. Natl. Acad. Sci. USA **110**: 12721–12726. doi: 10.1073/pnas.1216464110
- Mathis, J. T., J. N. Cross, and N. R. Bates. 2011. Coupling primary production and terrestrial runoff to ocean acidification and carbonate mineral suppression in the eastern Bering Sea. J. Geophys. Res. Oceans **116**: 1–24. doi: 10.1029/2010JC006453
- Mathis, J., J. Cross, W. Evans, and S. Doney. 2015. Ocean acidification in the surface waters of the Pacific-Arctic boundary regions. Oceanography **25**: 122–135. doi:10.5670/oceanog.2015.36
- Matson, P. G., L. Washburn, T. R. Martz, and G. E. Hofmann. 2014. Abiotic versus biotic drivers of ocean pH variation under Fast Sea Ice in McMurdo Sound. Antarctica **9**. doi: 10.1371/journal.pone.0107239
- McClelland, J. W., M. Stieglitz, F. Pan, R. M. Holmes, and B. J. Peterson. 2007. Recent changes in nitrate and dissolved organic carbon export from the upper Kuparuk River, North Slope, Alaska. J. Geophys. Res. Biogeosci. **112**: G04S60. doi: 10.1029/2006JG000371
- McClelland, J. W., R. M. Holmes, and K. H. Dunton. 2012. The Arctic Ocean estuary. Estuar. Coasts **35**: 353–368. doi: 10.1007/s12237-010-9357-3
- McClelland, J. W., A. Townsend-Small, R. M. Holmes, F. Pan, M. Stieglitz, M. Khosh, and B. J. Peterson. 2014. River export of nutrients and organic matter from the North Slope of Alaska to the Beaufort Sea. Water Resour. Res. **50**: 1823–1839. doi:10.1002/2013WR014722
- Mehrbach, C., C. H. Culberson, J. E. Hawley, and R. M. Pytkowicx. 1973. Measurement of the apparent dissociation constants of carbonic acid in seawater at atmospheric pressure. Limnol. Oceanogr. 18: 897–907. doi:10.4319/lo.1973.18.6.0897
- Meier, W. N., and others. 2014. Arctic Sea ice in transformation: A review of recent observed changes and impacts on biology and human activity. Rev. Geophys. **52**: 185–217. doi:10.1002/2013RG000431.Received
- Miller, C. A., K. Pocock, W. Evans, and A. L. Kelley. 2018. An evaluation of the performance of Sea-Bird Scientific's SeaFETTM autonomous pH sensor: Considerations for the

- broader oceanographic community. Ocean Sci. **14**: 751–768.
- Miller, L. A., T. M. Burgers, W. J. Burt, M. A. Granskog, and T. N. Papakyriakou. 2019. Air–sea CO₂ flux estimates in stratified Arctic coastal waters: How wrong can we be? Geophys. Res. Lett. **46**: 235–243. doi:10.1029/2018GL080099
- Miller, C. A., C. Bonsell, N. D. Mctigue, and A. L. Kelley. 2021. The seasonal phases of an Arctic lagoon reveal the discontinuities of pH variability and CO₂ flux at the air–sea interface. Biogeosciences **18**: 1203–1221. doi:10.5194/bg-18-1203-2021
- Morison, J., R. Kwok, C. Peralta-Ferriz, M. Alkire, I. Rigor, R. Andersen, and M. Steele. 2012. Changing Arctic Ocean freshwater pathways. Nature **481**: 66–70. doi:10.1038/nature10705
- Muth, A. F., A. J. Esbaugh, and K. H. Dunton. 2020. Physiological responses of an Arctic crustose coralline alga (*Leptophytum foecundum*) to variations in salinity. Front. Plant Sci. **11**: 1–10. doi:10.3389/fpls.2020.01272
- Muth, A. F., C. Bonsell, and K. H. Dunton. 2021. Inherent tolerance of extreme seasonal variability in light and salinity in an Arctic endemic kelp (*Laminaria solidungula*). J. Phycol. **1–9**: 1554–1562. doi:10.1111/jpy.13187
- Perry, H., C. Trigg, K. Larsen, J. Freeman, M. Erickson, and R. Henry. 2001. Calcium concentration in seawater and exoskeletal calcification in the blue crab, *Callinectes sapidus*. Aquaculture **198**: 197–208. doi:10.1016/S0044-8486(00) 00603-7
- Peterson, B. J., R. M. Holmes, J. W. McClelland, C. J. Vörösmarty, R. B. Lammers, A. I. Shiklomanov, and S. Rahmstorf. 2002. Increasing river discharge to the Arctic Ocean. Science **298**: 2171–2173. doi:10.1126/science.1077445
- Raven, J., and others. 2005. Ocean acidification due to increasing. *Coral Reefs*, June 12, 68 pp. Available from http://eprints.ifm-geomar.de/7878/1/965_Raven_2005_OceanAcidificationDueToIncreasing_Monogr_pubid13120.pdf
- Rember, R. D., and J. H. Trefry. 2004. Increased concentrations of dissolved trace metals and organic carbon during snowmelt in rivers of the Alaskan Arctic. Geochim. Cosmochim. Acta **68**: 477–489. doi:10.1016/S0016-7037 (03)00458-7
- Robbins, L. L., Hansen, M. E., Kleypas, J. A., & Meylan, S. C. 2010. CO2calc: A user-friendly seawater carbon calculator for Windows, Mac OS X, and iOS (iPhone). *In* Open-file report. 10.3133/ofr20101280
- Schneider, A., D. W. R. Wallace, and A. Körtzinger. 2007. Alkalinity of the Mediterranean Sea. Geophys. Res. Lett. **34**: 1–5. doi:10.1029/2006GL028842
- Sievers, J., L. L. Sørensen, T. Papakyriakou, B. Else, M. K. Sejr, D. H. Søgaard, and D. Barber. 2015. Winter observations of CO₂ exchange between sea ice and the atmosphere in a

coastal fjord environment. 1701–1713. Cryosphere **9**: 1701–1713. doi:10.5194/tc-9-1701-2015

- Tank, S. E., P. A. Raymond, R. G. Striegl, J. W. McClelland, R. M. Holmes, G. J. Fiske, and B. J. Peterson. 2012. A land-to-ocean perspective on the magnitude, source and implication of DIC flux from major Arctic rivers to the Arctic Ocean. Global Biogeochem. Cycles 26: 1–15. doi:10.1029/2011GB004192
- von Biela, V. R., C. E. Zimmerman, B. R. Cohn, and J. M. Welker. 2013. Terrestrial and marine trophic pathways support young-of-year growth in a nearshore Arctic fish. Polar Biol. **36**: 137–146. doi:10.1007/s00300-012-1244-x
- Weingartner, T. J., S. L. Danielson, R. A. Potter, J. H. Trefry, A. Mahoney, M. Savoie, and L. Sousa. 2017. Circulation and water properties in the landfast ice zone of the Alaskan Beaufort Sea. Cont. Shelf Res. **148**: 185–198. doi:10.1016/j. csr.2017.09.001
- Wickett, K., and Caldiera. 2003. Anthropogenic carbon and ocean pH. Nature **425**: 365. doi:10.1038/425365a
- Wilce, R. T., and K. H. Dunton. 2014. The Boulder Patch (North Alaska, Beaufort Sea) and its benthic algal flora. Arctic **67**: 43–56. doi:10.14430/arctic4360
- Yamamoto-Kawai, M., & Tanaka, N. 2005. Freshwater and brine behaviors in the Arctic Ocean deduced from historical data of 618O and alkalinity (1929–2002 AD). J. Geophys. Res. Oceans. **110**, 1–16. 10.1029/2004JC002793
- Yamamoto-Kawai, M., F. A. McLaughlin, E. C. Carmack, S. Nishino, and K. Shimada. 2009. Aragonite Undersaturation in the Arctic. Science 326: 1098–1100. doi:10.1126/science.1174190

Zhang, J. 2005. Warming of the arctic ice-ocean system is faster than the global average since the 1960s. Geophys. Res. Lett. **32**: 1–4. doi:10.1029/2005GL024216

Acknowledgments

This study was funded by the U.S. Department of Interior, Bureau of Ocean Energy and Management (BOEM), Alaska Outer Continental Shelf Region, Anchorage, Alaska under BOEM Cooperative Agreement No. M12AC00007 to K.H.D., STAR Fellowship Assistance Agreement no. FP917814 awarded by the U.S. Environmental Protection Agency (EPA) to A.F.M., and in kind support from the Beaufort Lagoon Ecosystems LTER program (National Science Foundation award OPP-1656026) to K.H.D. It has not been formally reviewed by E.P.A. The views expressed in this publication are solely those of A.F.M. and E.P.A. does not endorse any products or commercial services mentioned in this publication. Advice and help from E. Donham on pre-deployment set-up and troubleshooting throughout this process was invaluable. Thank you to C. Miller and M. DeGrandpre for edits on previous versions of this manuscript. We are extremely grateful to C. Bonsell, J. Dunton, and T. Dunton for their sustained contributions in the field, including vessel and dive support from the R.V. Proteus.

Conflict of Interest

Authors declare no conflicts of interests for this work and manuscript.

Submitted 25 June 2020 Revised 21 May 2021 Accepted 14 March 2022

Editor-in-Chief: K. David Hambright